Calpain Inhibition by α-Ketoamide and Cyclic Hemiacetal Inhibitors Revealed by X-ray Crystallography[†,‡]

D. Cuerrier,[§] T. Moldoveanu,[§,||] J. Inoue,[⊥] P. L. Davies,[§] and R. L. Campbell*[,§]

Department of Biochemistry, Queen's University, Kingston, Ontario, Canada K7L 3N6, and Research Laboratory, Senju Pharmaceutical Company, Ltd., 1-5-4 Murotani Nishi-ku, Kobe 651-2241, Japan

Received March 3, 2006; Revised Manuscript Received April 19, 2006

ABSTRACT: Calpains are intracellular calcium-activated cysteine proteases whose unregulated proteolysis following the loss of calcium homeostasis can lead to acute degeneration during ischemic episodes and trauma, as well as Alzheimer's disease and cataract formation. The determination of the crystal structure of the proteolytic core of μ-calpain (μI-II) in a calcium-bound active conformation has made structure-guided design of active site inhibitors feasible. We present here high-resolution crystal structures of rat μI-II complexed with two reversible calpain-specific inhibitors employing cyclic hemiacetal (SNJ-1715) and α-ketoamide (SNJ-1945) chemistries that reveal new details about the interactions of inhibitors with this enzyme. The SNJ-1715 complex confirms that the free aldehyde is the reactive species of the cornea-permeable cyclic hemiacetal. The α-ketoamide warhead of SNJ-1945 binds with the hydroxyl group of the tetrahedral adduct pointing toward the catalytic histidine rather than the oxyanion hole. The μI-II−SNJ-1945 complex shows residue Glu261 displaced from the S1′ site by the inhibitor, resulting in an extended "open" conformation of the domain II gating loop and an unobstructed S1′ site. This conformation offers an additional template for structure-based drug design extending to the primed subsites. An important role for the highly conserved Glu261 is proposed.

Calpains are a ubiquitous family of cysteine proteases found intracellularly, where they are involved in a wide range of physiological functions such as cell mobility, cell cycling, and transcriptional regulation (*1*). As they possess a calcium-dependent activity, they act by converting a local increase in calcium concentration into a proteolytic signal, resulting in the cleavage and altered function of target proteins. Calpain overactivation is associated with the pathogenesis of a wide range of disorders such as cataract formation, heart attack, stroke, Alzheimer's disease, and traumatic spinal cord and brain injury. Under these pathological conditions, a loss of calcium homeostasis within the cell results in the overactivation of and unregulated proteolysis by these calpains, where they contribute to the consequent cell and tissue damage. Calpains are therefore a valuable target for the development of drugs in the treatment of these conditions (*2*, *3*).

All currently known calpain isoforms are multidomain forms, and many are thought to be heterodimeric enzymes. The proteolytic active site is situated at the interface between papain-like domains I and II, which together form the proteolytic core of the enzyme. These domains contain two cooperative calcium-binding sites whose occupation is necessary for the rearrangement of the catalytic triad and the substrate binding site into an active conformation (*4*). The study of calpains in their native, full-length form is complicated by their susceptibility to autolysis, subunit dissociation, and aggregation upon Ca^{2+} activation (*5*). The proteolytic core of the enzyme, however, appears as a stable autolysis fragment that maintains (in the rat isoform) reduced but significant calcium-dependent proteolytic activity (*6*). Because of their stability, facile expression in heterologous *Escherichia coli* expression systems, and ease of crystallization, these isolated proteolytic cores or mini-calpains are currently the primary template onto which calpain structure-based drug design efforts are directed (*7*, *8*). This concept has been demonstrated by the determination of the crystal structures[1] of the proteolytic core of the rat μ-calpain isoform (μI-II) bound to the nonspecific protease inhibitors E-64[2] and leupeptin (*9*) and, more recently, human μI-II with a G213A stabilizing mutation (*10*) inactivated by ZLLY-CH_2F

[†] This work was funded by the Canadian Institutes for Health Research. D.C. is supported by a Natural Sciences and Engineering Research Council Studentship. T.M. is supported by a Canadian Institute of Health Research Postdoctoral Fellowship. P.L.D. holds a Canada Research Chair in Protein Engineering.

[‡] Coordinates and structure factors have been deposited with the Protein Data Bank as entries 2G8E and 2G8J.

* To whom correspondence should be addressed: Department of Biochemistry, Queen's University, Kingston, Ontario, Canada K7L 3N6. Telephone: (613) 533-6821. Fax: (613) 533-2497. E-mail: rlc1@post.queensu.ca.

[§] Queen's University.

[||] Current address: Department of Biochemistry, McGill University, Suite 5317, 3575 Avenue du Parc, Montreal, Quebec, Canada H2X 3P9.

[⊥] Senju Pharmaceutical Co., Ltd.

[1] The protein crystallographic structures mentioned in this paper can be found in the Protein Data Bank as entries 1TL9 (μI-II−leupeptin), 1TLO (μI-II−E-64), 1KXR (uncomplexed μI-II), 1ZCM (human μI-II−ZLLY-CH_2), 1DIT (thrombin−CVS995), 1TMB (thrombin−cyclotheonamide A), 1AHT (thrombin−α-keto acid), 1TPP (trypsin−α-keto acid), 1RGQ (HCV protease−α-ketoamide), 1DXW (HCV protease−α-keto acid), and 1YT7 and 1TU6 (cathepsin K−α-ketoamide).

[2] Abbreviations: DTT, D,L-dithiothreitol; E-64, *trans*-epoxysuccinyl-L-leucylamido(4-guanidino)butane; HEPES, 4-(2-hydroxyethyl)piperazine-1-ethanesulfonic acid; MES, 2-(*N*-morpholino)ethanesulfonic acid; Z-LLY-FMK, *N*-benzyloxycarbonyl-Leu-Leu-Tyr-fluoromethyl ketone.

10.1021/bi060425j CCC: $33.50
Published on Web 05/23/2006

(*11*). These structures have allowed the inhibitor interactions found in the active site binding pocket of calpain to be described. In addition, they revealed highly flexible gating loops, comprising residues 69−82 in domain I and 251−261 in domain II, that flank either side of the active site binding pocket and are thought to be involved in the binding and selectivity of protein substrates among various calpain isoforms.

Although they form potent serine and cysteine protease inhibitors as tetrahedral intermediate analogues, peptidyl aldehydes such as leupeptin and calpeptin have limited in vivo pharmacological value. The aldehyde group is thought to react with the nucleophilic amino or thiol groups of various biological substances, decreasing the bioavailability and cell permeability of the drug (*2*, *12*). One strategy for overcoming the chemical reactivity of the aldehyde is to "mask" it by providing an intramolecular site where it can react via reversible cyclic hemiacetal formation to a less reactive form. This strategy was previously applied in the design of 6-hydroxy-3-morpholinone calpain inhibitors, where the cyclic hemiacetal is formed through a hydroxyl group at the position otherwise occupied by the P2 amide (*12*) [nomenclature of Schecter and Berger (*13*)]. Similarly, other recently synthesized calpain inhibitors use a 2-hydroxytetrahydrofuran functionality, where formation of the cyclic hemiacetal occurs via a γ-hydroxyl group at P1 (*14*, *15*) (Figure 1A). In both cases, the free aldehyde form exists in equilibrium with its cyclic hemiacetal form, thus decreasing its total level of exposure and potential for side reactions.

Peptidyl α-ketoamides also exhibit improved metabolic stability compared to peptidyl aldehydes, and unlike α-keto acids and esters, they maintain their membrane permeability and are resistant to plasma esterases, although they typically are limited by low solubility (*16*−*18*). Also, unlike aldehydes and α-ketoacids that bind only the unprimed subsites, α-ketoamides can extend into the primed side of the active site.

The reversible calpain inhibitors SNJ-1715 (a cyclic hemiacetal) and SNJ-1945 (an α-ketoamide) were designed for use as anti-cataract and anti-retinopathy agents with improved bioavailability and corneal permeability (Figure 1A,B) (*14*, *19*). Both of these compounds demonstrate potent inhibition of m- and μ-calpain with IC_{50} values in the 86−190 nM range and exhibit efficacious anti-cataract properties in a rat lens culture model. Here we present the crystal structures of μI-II with these two inhibitors bound at the active site. These structures confirm the mode of action of the cyclic hemiacetal and reveal the interaction of calpain with an α-ketoamide warhead. The SNJ-1945-bound structure is the first instance of a calpain crystal structure with a ligand moiety stretching into the S1-primed subsite, resulting in an unobstructed binding pocket that suggests a potentially important switch mechanism involving the highly conserved Glu261. These structures should provide new opportunities and insights for designing potent and specific inhibitors for calpains.

EXPERIMENTAL PROCEDURES

Materials. Inhibitors SNJ-1715 and SNJ-1945 were synthesized as previously described (*14*, *19*). Stocks were prepared in 10 mM HEPES and 10 mM DTT and stored at

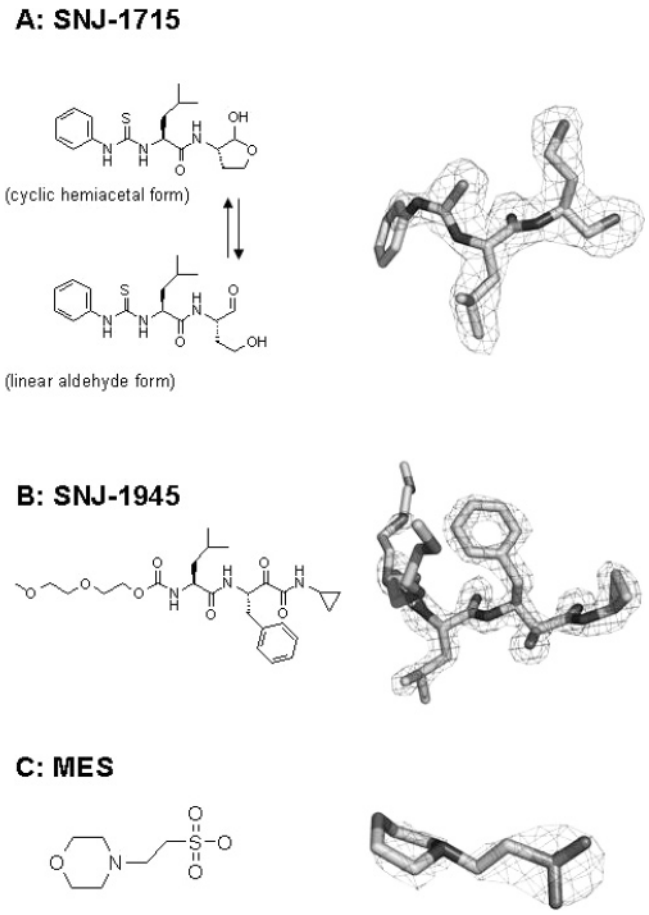

FIGURE 1: Chemical structures and fitted electron density of calpain inhibitors: (A) SNJ-1715, (B) SNJ-1945, and (C) crystallization buffer MES. The reversible intramolecular conversion of the cyclic hemiacetal of SNJ-1715 to the free aldehyde is shown. The observed electron density for the ligands is shown as a $F_o - F_c$ map calculated for the structures omitting the ligands and contoured at 3σ (SNJ-1715 and SNJ-1945) or 2σ (MES).

−20 °C. The μI-II construct is composed of Gly27−Asp356 from rat μ-calpain (calpain 1) with an N-terminal Met and a C-terminal Leu-Glu-$(His)_6$ tag. This construct was expressed and purified as previously described (*6*).

Determination of Crystal Structures of Complexes. A solution containing 13 mg/mL μI-II, 10 mM HEPES/NaOH (pH 7.6), and 10 mM DTT was preincubated in the presence of 0.6 mg/mL SNJ-1945 or 1.4 mg/mL SNJ-1715 for 1 h at room temperature in the absence of calcium, to ensure that the enzyme would be in the presence of inhibitor prior to activation by calcium. The crystals were obtained using the hanging drop vapor diffusion method by mixing the solution described above with an equal volume of a precipitant solution including conditions expanding around 1.1−1.7 M NaCl, 10 mM $CaCl_2$, and 0.1 M MES (pH 5.5−7.0). The crystals that were obtained were cryoprotected prior to data collection by being soaked in a solution of the mother liquor containing 15% glycerol. Data were collected on a Rigaku RU-200 rotating anode X-ray generator (50 kV and 100 mA), with an Osmic mirror system and a 300 mm image plate detector (MAR Research). The crystals were maintained at 100 K during data collection by a cryo-cooling system (Oxford Cryosystems). Data processing and manipulation were performed using Mosflm (*20*) and Scala of the CCP4 program suite (*21*). The inhibitor-complexed structures were

Table 1: Summary from Data Collection and Structure Refinement

	μI-II−SNJ-1715 complex[c]	μI-II−SNJ-1945 complex[c]
Crystal Parameters		
space group	$P4_322$	$P2_12_12_1$
a (Å)	85.54	40.57
b (Å)	85.54	70.40
c (Å)	117.95	110.90
Data Collection Statistics		
resolution range (Å)	2.25−19.7 (2.25−2.35)	1.61−59.4 (1.61−1.69)
no. of measured reflections	162137 (18138)	349474 (18891)
no. of unique reflections	21383 (2465)	39736 (5072)
completeness (%)	96.7 (78.2)	95.1 (82.9)
$I/\sigma I$	20.7 (5.4)	7.8 (3.9)
R_{merge}[a] (%)	8.4 (36.4)	6.9 (29.7)
Refined Structural Model		
resolution range (Å)	2.25−19.7 (2.25−2.31)	1.6−59.4 (1.61−1.66)
size of free reflection set (%)	5.1 (5.1)	5.0 (5.0)
R_{work}[b]	17.7 (19.5)	19.7 (31.4)
R_{free}	24.4 (22.7)	22.9 (36.4)
no. of protein/solvent/Ca^{2+} atoms (no H)	2640/205/2	2684/243/2
bond angle rmsd (deg)	1.755	1.268
bond length rmsd (Å)	0.02	0.011
average *B*-factor (Å^2)	26.4	16.0
B-factor from Wilson plot (Å^2)	32.7	16.4

[a] $R_{merge} = \sum|I_j - \langle I\rangle|/\sum I_j$, where I_j values are individual measurements for any reflection and $\langle I\rangle$ is the average intensity of the symmetry equivalent reflections. [b] $R_{cryst} = \sum|F_o - F_c|/\sum F_o$, where F_o and F_c are observed and calculated structure factor amplitudes, respectively. [c] Values in parentheses are for the outer resolution shell.

determined by molecular replacement using MOLREP (*22*) with the native holo-μI-II (chain A of PDB entry 1KXR) as the model. The refinement of the model was done using REFMAC5 (*23*), while XtalView/XFit (*24*) was used for model building. The Dundee PRODRG2 server (*25*) was used to generate the molecular topology description of the ligand. All structure diagrams were generated in PyMOL (*26*).

RESULTS

Although crystallized under similar conditions, the calpain−inhibitor complexes presented here crystallized in different space groups. The SNJ-1715 complex exhibited $P4_322$ symmetry, and the SNJ-1945 complex exhibited $P2_12_12_1$ symmetry, both with a single molecule present in the asymmetric unit (Table 1). Despite the different space groups, the two μI-II structures exhibit a high degree of similarity between their α-carbon backbones (rmsd = 0.36 Å) and with previously determined structures of free and complexed μI-II (*9*). Both inhibitors were observed as electron densities stretching along the S-unprimed subsites of the enzyme (Figure 1A,B), with the density for the SNJ-1715 complex clearly corresponding to the hemithioacetal of the free aldehyde rather than the cyclic hemiacetal. In the S-primed subsites of the SNJ-1715 complex, electron density with a morphology matching that of a molecule of the crystallization buffer MES [2-(*N*-morpholino)ethanesulfonic acid] was also fitted (Figure 1C).

The P3 diethylene glycol group of SNJ-1945 shows weak electron density, indicative of high flexibility and minimal interactions with the binding site, consistent with its role in improving the bioavailability and solubility of the compound without significantly impacting inhibitory potency (*19*). Two potential conformers of this group were fitted. Both the higher-occupancy conformer of the diethylene glycol of SNJ-1945 and the P3 phenylthiourea group of SNJ-1715 lie along the surface of domain I (Figure 2), as do the P3 leucyl and 4-guanidinobutane group of leupeptin and E-64 in their respective complexed structures (*9*), suggesting that this is the site to which the P3 group of most inhibitors should be directed.

Both of the SNJ-1715 and SNJ-1945 complexes have hydrogen bonds formed between the peptidyl backbone of the inhibitor (carbonyl oxygen and amide nitrogen of the P2 residue and the amide nitrogen of the P1 residue) and residues Gly271 and Gly208 of the active site binding pocket (Figure 3). These hydrogen bonds are conserved in the leupeptin- and ZLLY-CH_2-bound structures and likely represent canonical interactions that are also formed with the peptide backbone of a substrate.

The P2 leucine side chains of both inhibitors fit within the S2 hydrophobic pocket in an identical conformation as observed in the leupeptin complex (Figure 2). The positions of the backbone and side chain of the P2 Leu as well as the backbone and side chain β- and γ-carbons of the P1 Phe/homo-Ser align almost perfectly with each other and with the corresponding atoms of leupeptin (P2 Leu and P1 Arg) in its complex with μI-II. The high degree of structural alignment of the P1 side chains appears to be due to a shallow pocket formed by the backbone Cα of Gly113 that restricts the rotation of the P1 residue around the χ_1 (Cα−Cβ) bond in one direction (for both the SNJ-1715- and SNJ-1945-complexed structure) and the Leu260 side chain in the domain II gating loop in the other direction (for the SNJ-1715-complexed structure only).

The aldehyde warhead of SNJ-1715 interacts with the active site in a manner identical to that of leupeptin's aldehyde warhead by forming a stable hemithioacetal bond with the catalytic cysteine (*9*), with the resulting hydroxyl group pointing toward the oxyanion hole formed by the side chain of Gln109 and the backbone amide nitrogen of Cys115 (Figure 3). The α-ketoamide warhead of SNJ-1945 also acts

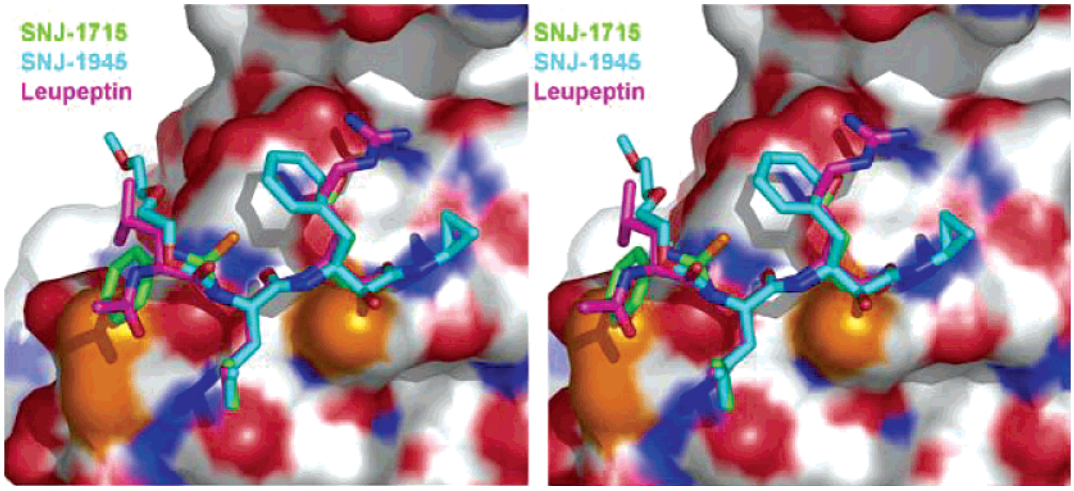

FIGURE 2: Structural overlap of three calpain inhibitors. The overlap of leupeptin, SNJ-1945, and SNJ-1715 was obtained from the structural alignment of the polypeptide chain of each structure. Inhibitors are shown in stick representations, with carbon atoms colored as follows: magenta for leupeptin, cyan for SNJ-1945, and green for SNJ-1715. A surface representation of μI-II domain I from the SNJ-1945 complex is shown with carbons in white, nitrogens in blue, and oxygens in red. Domain II and the low-occupation conformer of the ethylene glycol chain of SNJ-1945 were omitted for clarity.

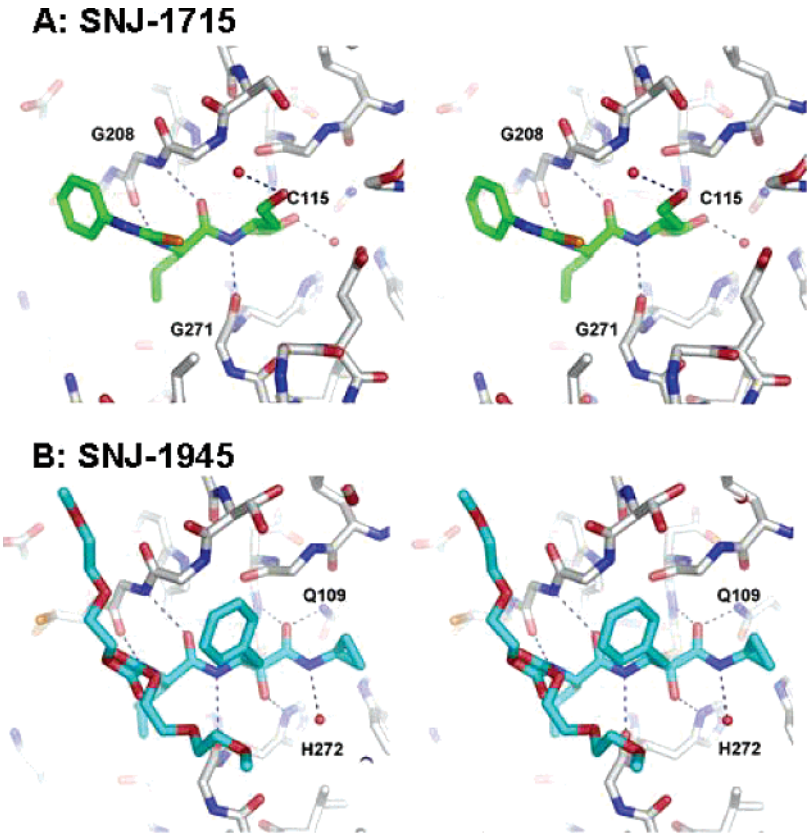

FIGURE 3: Hydrogen bonding interactions between μI-II and its inhibitors. All intermolecular polar interactions between μI-II and (A) SNJ-1715 and (B) SNJ-1945 of <3 Å are shown. Carbon atoms are colored as in Figure 2, with water molecules shown as small red spheres. The two images are shown in the same orientation.

as an analogue of the tetrahedral intermediate but forms a larger number of significant polar contacts to stabilize the bound form of the inhibitor. The position of the α-ketoamide adduct within the active site indicates that covalent attachment of the inhibitor arises from the nucleophilic attack of the activated thiol on the *re* face of the α-keto carbonyl, with His272 subsequently donating a proton to the oxyanion of the tetrahedral adduct. The resulting hydroxyl group remains stabilized by a potentially strong hydrogen bond to Nδ1 of His272 (2.7 Å) and a presumed weaker hydrogen bond to the backbone oxygen of Gly271 (3.1 Å), forming a stably trapped intermediate. The carbonyl oxygen of the carboxyamide further stabilizes this trapped intermediate through two hydrogen bonds with the canonical oxyanion hole consisting of Gln109 and Cys115. The hydrogen bonds formed with the oxyanion holes are shorter for the carboxyamide of SNJ-1945 (2.7 and 2.8 Å to the Nϵ2 atom of Gln109 and the backbone amide nitrogen of Cys115, respectively) than for the hydroxyl group formed by the aldehyde warhead of SNJ-1715 (3.4 and 3.2 Å, respectively),

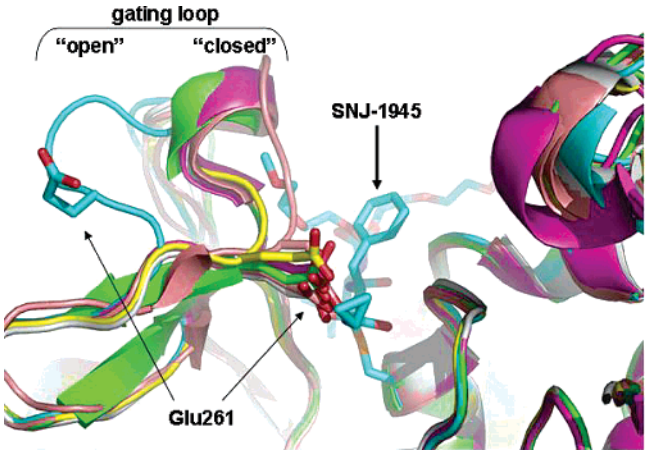

FIGURE 4: Displacement of Glu261 by the P1′-cyclopropyl group in the SNJ-1945-bound structure. The polypeptide portions of six μI-II structures are shown superimposed. Inhibitor SNJ-1945 bound to Cys115 is shown as sticks, along with the side chain of Glu261 from all six structures. The gating loop (residues 251−261) appears in a "closed" conformation with Glu261 obstructing the S1′ subsite in five of the six structures but in an "open" conformation with a displaced Glu261 in the SNJ-1945-bound structure (cyan). The polypeptides are colored as follows: cyan for the SNJ-1945 complex, green for the SNJ-1715 complex, magenta for the leupeptin complex, yellow for the E-64 complex, salmon for the uncomplexed μI-II C115S, and white for the Z-LLY-FMK−human μI-II complex.

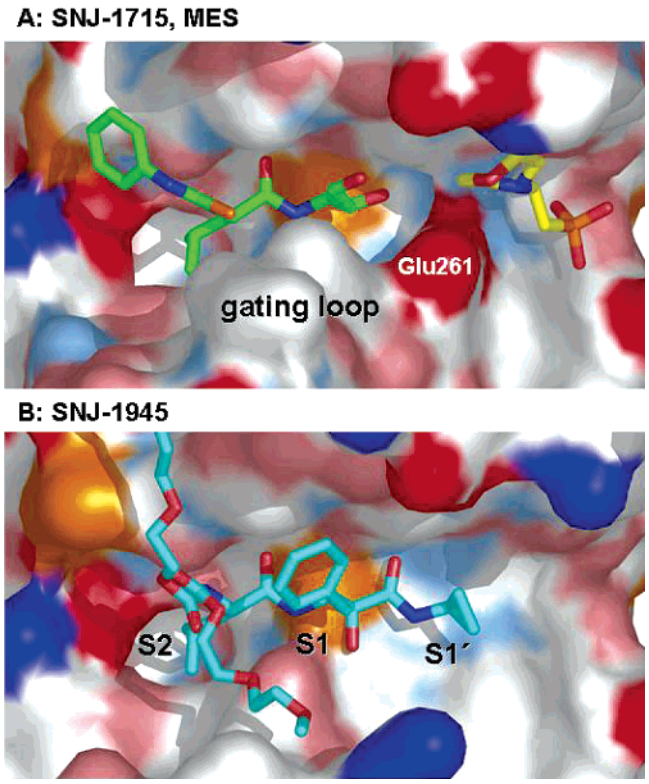

FIGURE 5: Active site binding pocket of μI-II bound to SNJ-1715 and SNJ-1945. (A) The SNJ-1715 complex (with a MES molecule occupying the S′ subsites) displays a closed gating loop with Glu261 obstructing the S1′ site. (B) Conversely, the SNJ-1945-bound structure displays an open S1′ subsite. The ligand atoms are shown as sticks of the same color as in Figure 2, with MES carbon atoms colored yellow. The enzyme is shown in surface representation with carbons in white, sulfur in orange, charged oxygens in dark red, uncharged oxygens in light red, charged nitrogens in dark blue, and uncharged nitrogens in light blue. Both figures are shown in the same orientation.

suggesting a stronger interaction in the former. The amide nitrogen of the SNJ-1945 warhead is not observed to form any polar interactions with μI-II but forms a hydrogen bond with crystallographic water HOH57 (2.9 Å).

The cyclopropyl ring of SNJ-1945 extends into the S-primed subsites from a shallow cleft formed by the indole ring of Trp298, Cα of Gly113, and the side chain of Gln109. This cleft is not observed in the uncomplexed, SNJ-1715-bound, or leupeptin-bound structures of μI-II due to the presence of Glu261 in the cleft (Figure 4). The gating loop containing residues 256−261 has little density for the backbone and side chain atoms of the SNJ-1945-bound structure, indicating a high degree of flexibility in this region. The location of these residues was fit to what density was present. In contrast, the backbone atoms of residues 256−261, including the side chain atoms of Glu261, are fairly well defined in the SNJ-1715-bound structure despite the absence of stabilizing interactions from the crystal packing.

DISCUSSION

Calpain inhibitor SNJ-1715 was designed with a 2-hydroxytetrahydrofuran warhead to mask the reactivity of its aldehyde and improve permeability and bioavailability (*14*, *15*) (Figure 1A). The electron density found at the active site of the SNJ-1715-bound structure unambiguously corresponds to the hemithioacetal of an aldehyde warhead with a P1 homoserine residue, thus confirming that the reactive species of the cyclic hemiacetal is the free aldehyde.

Interestingly, the adduct formed from the α-ketoamide warhead of SNJ-1945 and the protease core of rat μ-calpain has the hydroxyl of the tetrahedral adduct pointing toward the catalytic histidine rather than the oxyanion hole, which is occupied by the carboxyamide oxygen (Figure 3B). Inspection of the crystal structures of other protease−α-keto inhibitor complexes deposited in the Protein Data Bank revealed that two cysteine protease−α-ketoamide complexes of cathepsin K as well as an α-ketoamide and an α-keto acid complex with the hepatitis C NS3 serine protease show the warhead adopting a binding mode similar to that observed with the calpain−SNJ-1945 complex (*27*−*30*). Conversely, the serine proteases thrombin and trypsin in complex with α-ketoamide and α-keto acid inhibitors consistently show the hydroxyl group of the tetrahedral adduct stabilized by the canonical oxyanion hole of serine proteases (formed by the backbone N atoms of the catalytic Ser195 and Gly193) and the carboxyamide oxygen pointed toward the imidazolium group of the catalytic histidine (*31*−*34*). This suggests a difference in the mode of binding of the α-ketoamide warhead to proteases of different families, depending on which face of the electrophilic ketone produces a stable intermediate upon attack by the thiolate. This specificity for a particular binding mode could potentially be exploited to increase the selectivity of α-ketoamide inhibitors.

In previously determined μI-II structures, residues 251−261 of domain II form a flexible loop with variable (but typically low) electron density known as the gating loop (*9*, *11*). This region is usually modeled with a conformation similar to that observed in the SNJ-1715-bound structure, with residue Glu261 occupying the S1′ subsite in the binding cleft (Figures 4 and 5A). Whereas this loop shows reasonably well-defined density in the SNJ-1715-bound structure, in the

FIGURE 6: Conservation of Glu261 within the catalytic subunit of calpain isoforms. The sequence of residues 234−286 (from helix 7 to β-strand 11 inclusive) from rat μ-calpain (r-CAPN1) was aligned with the sequence of other calpain isoforms from human (h-), rat (r-), *Drosophila melanogaster* (Dm-), and *Caenorhabditis elegans* (Ce-) using ClustalW (*38*). The accession numbers for each isoform are AAH61880 (r-CAPN1), AAH75862 (h-CAPN1), AAH11828 (h-CAPN2), P20807 (h-CAPN3), AAH18123 (h-CAPN5), AAH00730 (h-CAPN6), AAH56202 (h-CAPN7), NP_579843 (r-CAPN8), AAW49735 (h-CAPN9), Q9HC96 (h-CAPN10), AAH33733 (h-CAPN11), Q6ZSI9 (h-CAPN12), NP_653176 (h-CAPN13), CAA86993 (Dm-calpA), and Q22036 (Ce-tra3). The level of identity between isoforms is indicated in black (100%), dark gray (75−100%), and light gray (50−75%). The arrow points to the highly conserved Glu261 residue. The black bar corresponds to the flexible gating loop in domain II. The central region (44 residues) of the insertion sequence of calpain 3 (hCAPN3) has been omitted (*).

SNJ-1945-bound structure the P1′ cyclopropyl moiety of the inhibitor occupies the position of the Glu261 side chain in previous structures (Figures 4 and 5B), and little density is observed for residues 256−261. This suggests that the P1′ cyclopropyl displaces Glu261 from the S1′ site, resulting in an extended flexibility of the gating loop and a structure with a conformation much more open than that previously observed. The conservation of Glu261 within human calpain isoforms and those of other organisms, further emphasized by its location adjacent to a nonconserved region of domain II, suggests that it has a critical functional role in calpains (Figure 6). One possible role is the involvement of this residue in signaling the presence of a substrate bound to the active site, possibly via interactions that require other domains not present in the isolated proteolytic core. A second possibility is that the residue is designed to either promote or hinder catalysis, possibly by interacting with the acyl−enzyme intermediate.

The displacement of Glu261 from the S1′ site creates an active site cleft that is more open and more representative of a substrate-bound conformation of the enzyme (Figure 5B). The SNJ-1945-bound model is therefore of great value for the structure-based design of fragments extending to primed subsites. One of the difficulties encountered in the development of therapeutically viable active site-directed inhibitors for calpains is the lack of target specificity relative to other intracellular cysteine proteases, such as cathepsins B and L, that have P1 and P2 preferences similar to those of calpains (*35*). We have recently shown that primed side interactions are important determinants in the calpain hydrolysis of peptide substrates (*36*). Designing inhibitors that interact with primed subsites is a potential tactic for improving calpain specificity that remains to be fully exploited. Although this is the first reported structure of the active site of calpain with an inhibitor that extends into the S-primed subsites, the cyclopropyl group at S1′ has only a limited potential for interactions. Previous work on an inhibitor series exhibiting a structure very similar to that of SNJ-1945 has shown that the presence of a secondary amine in place of the cyclopropyl ring increased the potency of inhibition by greater than 10-fold (*8*). From the structure of the SNJ-1945 complex, this secondary amine would be in a position to interact with the carbonyl oxygen from the Leu112 backbone.

The presence of a MES molecule in the S-primed binding subsites of the μI-II−SNJ-1715 complex (Figure 5A) is likely an artifact of crystallization in the $P4_322$ space group, as the electron density is relatively weak and there are no reports that MES buffer acts as a competitive inhibitor of calpains. Nonetheless, it suggests a potential functional group that is structurally complementary with the primed subsites. Indeed, calpain inhibitor AK-295 was designed with a MES-like morpholinopropyl moiety at P1′ that was found to increase the solubility of the compound relative to that of the analogous compound with a P1′-ethyl (AK-275) while preserving the potency and selectivity of the inhibitor (*37*). Though the lack of polar interactions suggests a structural complementarity that may be generalized to a cyclohexyl group, the wide open cleft in the primed subsites suggests a large variety of structures may otherwise occupy this position.

In conclusion, we have illustrated how the determination and scrutiny of calpain−inhibitor complexes can lead to insight that may be applied to the design of calpain-specific inhibitors. To further generalize and improve the knowledge base of calpain−inhibitor interactions necessary for structure-based drug design, the need for more experimentally determined calpain structures, especially with fragments that extend into S-primed subsites, is evident. The SNJ-1945-bound structure highlights a novel movement of the gating loop to give an open conformation of the primed side binding pocket as a result of a substrate or inhibitor fragment occupying primed subsites. This high-resolution structure provides a significant improvement over previous modeling templates for primed side extending inhibitors of calpains and should contribute greatly to the field of structure-based drug design for these pathologically important enzymes.

ACKNOWLEDGMENT

We are grateful to Dr. Zongchao Jia (Department of Biochemistry, Queen's University) for providing the facilities for X-ray crystallography data collection.

REFERENCES

1. Goll, D. E., Thompson, V. F., Li, H., Wei, W., and Cong, J. (2003) The Calpain System, *Physiol. Rev. 83*, 731−801.
2. Wang, K. K., and Yuen, P. W. (1997) Development and therapeutic potential of calpain inhibitors, *Adv. Pharmacol. 37*, 117−152.
3. Carragher, N. O. (2006) Calpain inhibition: A therapeutic strategy targeting multiple disease states, *Curr. Pharm. Des. 12*, 615−638.
4. Moldoveanu, T., Jia, Z., and Davies, P. L. (2004) Calpain activation by cooperative Ca^{2+} binding at two non-EF-hand sites, *J. Biol. Chem. 279*, 6106−6114.
5. Pal, G. P., Elce, J. S., and Jia, Z. (2001) Dissociation and aggregation of calpain in the presence of calcium, *J. Biol. Chem. 276*, 47233−47238.
6. Moldoveanu, T., Hosfield, C. M., Lim, D., Elce, J. S., Jia, Z., and Davies, P. L. (2002) A Ca^{2+} switch aligns the active site of calpain, *Cell 108*, 649−660.
7. Neffe, A. T., and Abell, A. D. (2005) Developments in the design and synthesis of calpain inhibitors, *Curr. Opin. Drug Discovery Dev. 8*, 684−700.
8. Donkor, I. O., Han, J., and Zheng, X. (2004) Design, synthesis, molecular modeling studies, and calpain inhibitory activity of novel α-ketoamides incorporating polar residues at the P1′-position, *J. Med. Chem. 47*, 72−79.
9. Moldoveanu, T., Campbell, R. L., Cuerrier, D., and Davies, P. L. (2004) Crystal structures of calpain-E64 and -leupeptin inhibitor complexes reveal mobile loops gating the active site, *J. Mol. Biol. 343*, 1313−1326.
10. Moldoveanu, T., Hosfield, C. M., Lim, D., Jia, Z., and Davies, P. L. (2003) Calpain silencing by a reversible intrinsic mechanism, *Nat. Struct. Biol. 10*, 371−378.
11. Li, Q., Hanzlik, R. P., Weaver, R. F., and Schonbrunn, E. (2006) Molecular mode of action of a covalently inhibiting peptidomimetic on the human calpain protease core, *Biochemistry 45*, 701−708.
12. Nakamura, M., Miyashita, H., Yamaguchi, M., Shirasaki, Y., Nakamura, Y., and Inoue, J. (2003) Novel 6-hydroxy-3-morpholinones as cornea permeable calpain inhibitors, *Bioorg. Med. Chem. 11*, 5449−5460.
13. Schechter, I., and Berger, A. (1967) On the size of the active site in proteases. I. Papain, *Biochem. Biophys. Res. Commun. 27*, 157−162.
14. Nakamura, M., Yamaguchi, M., Sakai, O., and Inoue, J. (2003) Exploration of cornea permeable calpain inhibitors as anticataract agents, *Bioorg. Med. Chem. 11*, 1371−1379.
15. Auvin, S., Pignol, B., Navet, E., Pons, D., Marin, J. G., Bigg, D., and Chabrier, P. E. (2004) Novel dual inhibitors of calpain and lipid peroxidation, *Bioorg. Med. Chem. Lett. 14*, 3825−3828.
16. Li, Z., Patil, G. S., Golubski, Z. E., Hori, H., Tehrani, K., Foreman, J. E., Eveleth, D. D., Bartus, R. T., and Powers, J. C. (1993) Peptide α-keto ester, α-keto amide, and α-keto acid inhibitors of calpains and other cysteine proteases, *J. Med. Chem. 36*, 3472−3480.
17. Harbeson, S. L., Abelleira, S. M., Akiyama, A., Barrett, R., III, Carroll, R. M., Straub, J. A., Tkacz, J. N., Wu, C., and Musso, G. F. (1994) Stereospecific synthesis of peptidyl α-keto amides as inhibitors of calpain, *J. Med. Chem. 37*, 2918−2929.
18. Lescop, C., Herzner, H., Siendt, H., Bolliger, R., Hennebohle, M., Weyermann, P., Briguet, A., Courdier-Fruh, I., Erb, M., Foster, M., Meier, T., Magyar, J. P., and von Sprecher, A. (2005) Novel cell-penetrating α-keto-amide calpain inhibitors as potential treatment for muscular dystrophy, *Bioorg. Med. Chem. Lett. 15*, 5176−5181.
19. Shirasaki, Y., Miyashita, H., Yamaguchi, M., Inoue, J., and Nakamura, M. (2005) Exploration of orally available calpain inhibitors: Peptidyl α-ketoamides containing an amphiphile at P3 site, *Bioorg. Med. Chem. 13*, 4473−4484.
20. Leslie, A. G. W. (1992) Recent changes to the MOSFLM package for processing film and image plate data, *Joint CCP4 and ESF-EAMCB Newsletter on Protein Crystallography 26*.
21. Potterton, E., McNicholas, S., Krissinel, E., Cowtan, K., and Noble, M. (2002) The CCP4 molecular-graphics project, *Acta Crystallogr. D58*, 1955−1957.
22. Vagin, A. T. (1997) MOLREP: An automated program for molecular replacement, *J. Appl. Crystallogr. 30*, 1022−1025.
23. Murshudov, G. N., Vagin, A. A., Lebedev, A., Wilson, K. S., and Dodson, E. J. (1999) Efficient anisotropic refinement of macromolecular structures using FFT, *Acta Crystallogr. D55* (Part 1), 247−255.
24. McRee, D. E. (1999) XtalView/Xfit: A versatile program for manipulating atomic coordinates and electron density, *J. Struct. Biol. 125*, 156−165.
25. Schuttelkopf, A. W., and van Aalten, D. M. (2004) PRODRG: A tool for high-throughput crystallography of protein−ligand complexes, *Acta Crystallogr. D60*, 1355−1363.
26. DeLano, W. L. (2003) *PyMol*, DeLano Scientific LLC, San Carlos, CA.
27. Barrett, D. G., Boncek, V. M., Catalano, J. G., Deaton, D. N., Hassell, A. M., Jurgensen, C. H., Long, S. T., McFadyen, R. B., Miller, A. B., Miller, L. R., Payne, J. A., Ray, J. A., Samano, V., Shewchuk, L. M., Tavares, F. X., Wells-Knecht, K. J., Willard, D. H., Jr., Wright, L. L., and Zhou, H. Q. (2005) P2−P3 conformationally constrained ketoamide-based inhibitors of cathepsin K, *Bioorg. Med. Chem. Lett. 15*, 3540−3546.
28. Barrett, D. G., Catalano, J. G., Deaton, D. N., Hassell, A. M., Long, S. T., Miller, A. B., Miller, L. R., Shewchuk, L. M., Wells-Knecht, K. J., Willard, D. H., Jr., and Wright, L. L. (2004) Potent and selective P2−P3 ketoamide inhibitors of cathepsin K with good pharmacokinetic properties via favorable P1′, P1, and/or P3 substitutions, *Bioorg. Med. Chem. Lett. 14*, 4897−4902.
29. Barbato, G., Cicero, D. O., Cordier, F., Narjes, F., Gerlach, B., Sambucini, S., Grzesiek, S., Matassa, V. G., De Francesco, R., and Bazzo, R. (2000) Inhibitor binding induces active site stabilization of the HCV NS3 protein serine protease domain, *EMBO J. 19*, 1195−1206.
30. Liu, Y., Stoll, V. S., Richardson, P. L., Saldivar, A., Klaus, J. L., Molla, A., Kohlbrenner, W., and Kati, W. M. (2004) Hepatitis C NS3 protease inhibition by peptidyl-α-ketoamide inhibitors: Kinetic mechanism and structure, *Arch. Biochem. Biophys. 421*, 207−216.
31. Krishnan, R., Tulinsky, A., Vlasuk, G. P., Pearson, D., Vallar, P., Bergum, P., Brunck, T. K., and Ripka, W. C. (1996) Synthesis, structure, and structure−activity relationships of divalent thrombin inhibitors containing an α-keto-amide transition-state mimetic, *Protein Sci. 5*, 422−433.
32. Maryanoff, B. E., Qiu, X., Padmanabhan, K. P., Tulinsky, A., Almond, H. R., Jr., Andrade-Gordon, P., Greco, M. N., Kauffman, J. A., Nicolaou, K. C., Liu, A., et al. (1993) Molecular basis for the inhibition of human α-thrombin by the macrocyclic peptide cyclotheonamide A, *Proc. Natl. Acad. Sci. U.S.A. 90*, 8048−8052.
33. Walter, J., and Bode, W. (1983) The X-ray crystal structure analysis of the refined complex formed by bovine trypsin and p-amidinophenylpyruvate at 1.4 Å resolution, *Hoppe-Seyler's Z. Physiol. Chem. 364*, 949−959.
34. Chen, Z., Li, Y., Mulichak, A. M., Lewis, S. D., and Shafer, J. A. (1995) Crystal structure of human α-thrombin complexed with hirugen and p-amidinophenylpyruvate at 1.6 Å resolution, *Arch. Biochem. Biophys. 322*, 198−203.
35. Choe, Y., Leonetti, F., Greenbaum, D. C., Lecaille, F., Bogyo, M., Bromme, D., Ellman, J. A., and Craik, C. S. (2006) Substrate profiling of cysteine proteases using a combinatorial peptide library identifies functionally unique specificities, *J. Biol. Chem. 281*, 12824−12832.
36. Cuerrier, D., Moldoveanu, T., and Davies, P. L. (2005) Determination of peptide substrate specificity for μ-calpain by a peptide library-based approach: The importance of primed side interactions, *J. Biol. Chem. 280*, 40632−40641.
37. Bartus, R. T., Hayward, N. J., Elliott, P. J., Sawyer, S. D., Baker, K. L., Dean, R. L., Akiyama, A., Straub, J. A., Harbeson, S. L., Li, Z., et al. (1994) Calpain inhibitor AK295 protects neurons from focal brain ischemia. Effects of postocclusion intra-arterial administration, *Stroke 25*, 2265−2270.
38. Thompson, J. D., Higgins, D. G., and Gibson, T. J. (1994) CLUSTAL W: Improving the sensitivity of progressive multiple sequence alignment through sequence weighting, position-specific gap penalties and weight matrix choice, *Nucleic Acids Res. 22*, 4673−4680.

BI060425J